

The Kinematics of Galactic Stellar Disks

Michael R. Merrifield

*Department of Physics & Astronomy, University of Southampton,
Highfield, Southampton, SO17 1BJ, England*

Konrad Kuijken

Kapteyn Instituut, PO Box 800. 9700 AV Groningen, The Netherlands

Abstract. The disks of galaxies are primarily stellar systems, and fundamentally dynamical entities. Thus, to fully understand galactic disks, we must study their stellar kinematics as well as their morphologies. Observational techniques have now advanced to a point where quite detailed stellar-kinematic information can be extracted from spectral observations. This review presents three illustrative examples of analyses that make use of such information to study the formation and evolution of these systems: the derivation of the pattern speed of the bar in NGC 936; the calculation of the complete velocity ellipsoid of random motions in NGC 488; and the strange phenomenon of counter-rotation seen in NGC 3593.

1. Introduction

Disk galaxies, with their pleasing symmetry and intricate spiral structure, are amongst the most beautiful of astronomical objects. They owe this beauty to two basic factors. First, and fairly obviously, they are visible to us because they are made up of stars emitting at optical wavelengths. Second, they are fundamentally dynamical entities. As first recognized by Immanuel Kant, their basic disk shapes arise from the ordered angular momenta of their constituent stars. Even the finer detail of spiral arms, bars, rings, and so on, can only be understood in terms of the collective motions of stars.

The stellar motions also provide a key to studying the formation and evolution of galaxies. The two-body relaxation time for close encounters between stars to significantly re-arrange their orbits is $\sim 10^{16}$ years. Thus, the only processes that can affect the arrangement of stellar orbits are the original formation of the galaxy, and any large-scale collective phenomena such as those produced by dynamical instabilities or interactions with other galaxies. By studying the arrangement of orbits in a galaxy, we are tapping directly into the archaeological record of these processes.

Finally, it should be remembered that the observed stellar component is the tip of the galactic iceberg: the total mass of galaxies seems to be dominated by non-luminous “dark matter.” Since the gravitational potential dictating the stars’ orbits is generated by all the mass in the galaxy, the arrangement of

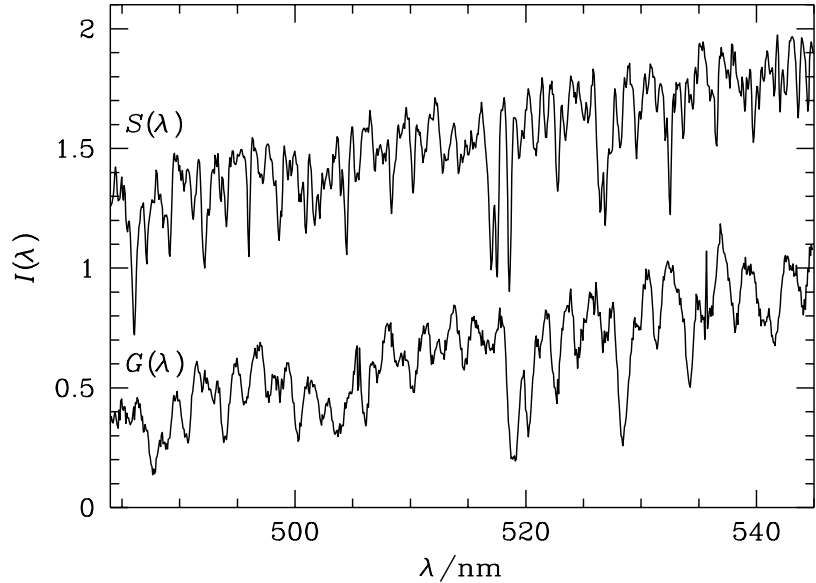


Figure 1. Intensity as a function of wavelength for a K0 giant star [$S(\lambda)$] and a small part of a galaxy [$G(\lambda)$]. The strong absorption lines at ~ 517 nm are the Mg b feature, and most of the other lines are due to Fe. Note the Doppler broadening and shift in the galaxy spectrum. [Reproduced from Binney & Merrifield (1998).]

stellar orbits provides one of the few direct mechanisms by which we can “see” this invisible component. The simplest analyses involve deriving the over-all distribution of mass in a galaxy from the circular motions of stars around the disk at different radii (e.g. Kent 1987). However – as we shall see in Section 2 – it is also possible to draw subtler inferences about the distribution of dark matter in disk galaxies from the systems’ stellar-kinematic properties.

Thus, if we want to understand the formation and evolution of disk galaxies, and probe the underlying distribution of mass in such systems, we need to investigate the motions of their constituent stars. The primary technique for studying such motions is through the Doppler shifts of the absorption lines in the stars’ spectra. Unfortunately, we cannot observe individual stars in any but the closest of galaxies; typically, a spectrum of the smallest resolvable element of a galaxy will contain the light from hundreds of thousands of stars. However, there is still plenty of dynamical information in the composite galaxy spectrum: the spectrum of each contributing star will be Doppler shifted by a slightly different amount, so the absorption lines in the integrated spectrum will be significantly broader than those in a stellar spectrum (see Figure 1). In fact, if we assume that all the stars in the galaxy have identical spectra, then the observed galaxy spectrum will be simply a convolution of the stellar spectrum with a broadening function that represents the distribution of line-of-sight velocities of all the stars that contribute to the light. Thus, if we obtain both a galaxy and a stellar spectrum, we can derive the line-of-sight-velocity distribution of the stars in the galaxy spectrum through a process of deconvolution.

In practice, extracting this dynamical information is not a trivial process. First, galactic disks are intrinsically faint objects: in their most luminous central regions, they are only comparable to the brightness of the night sky. Thus, it is difficult and time consuming to obtain galaxy spectra at even moderate signal-to-noise ratios. However, the development of high-throughput spectrographs and efficient detectors has made it possible to dramatically improve the quality of galactic spectra that can be attained, and the arrival of 8m-class telescopes will make such data routinely available.

The second problem is that the deconvolution process greatly amplifies any noise in the data. Hence, even a galaxy spectrum of high quality will only yield a very poor estimate for the distribution of stellar velocities unless some care is taken. The traditional solution to this problem has been to assume that the stellar line-of-sight velocity distribution has a particularly simple form, which is usually taken to be a Gaussian (e.g. Sargent et al. 1977, Tonry & Davis 1979). The kinematics of the galaxy are then quantified by finding the best-fit Gaussian such that, when the stellar spectrum is convolved with this distribution, the resulting broadened spectrum most closely matches the galaxy data. The mean of the Gaussian then provides a measure of the mean streaming motion of the stars, while its dispersion quantifies the stellar random motions. More recently, algorithms have been developed that allow a more general deconvolution of spectral data without uncontrollable amplification of the noise (e.g. Gerhard 1993, van der Marel & Franx 1993, Kuijken & Merrifield 1993). Using such techniques, it is now possible to go beyond the traditional crude measures of stellar kinematics to estimate the complete line-of-sight velocity distribution of all the stars that contribute to a galaxy spectrum.

In this review, we present the results of three recent projects that investigate the dynamics of stellar disks. These examples are not intended to provide a comprehensive overview of current work on stellar disk dynamics; rather, they have been chosen simply to illustrate the variety of information that can be gleaned from such studies. Section 2. describes the calculation of the pattern speed of the bar in NGC 936 from the stellar mean streaming motions in this galaxy. As we discuss, in addition to being a fundamental property of barred galaxies, the derived pattern speed also has implications for the distribution of dark matter in galaxies. The second example, presented in Section 3., shows how the three-dimensional distribution of random motions within the disk galaxy NGC 488 can be derived from the broadening of its spectral lines, and how the balance between the velocity dispersions in different directions can be used to identify the “heating” process responsible for producing these random motions. Finally, Section 4. illustrates the strange phenomenon of counter-rotation detected in a few stellar disks by presenting the complete line-of-sight velocity distribution for the stars in the edge-on disk galaxy NGC 3593.

2. The Pattern Speed of NGC 936

Approximately a third of disk galaxies contain a central rectangular enhancement in their stellar densities (see Figure 2, left panel). It has long been recognized that such stellar bars are the product of a dynamical instability in self-gravitating disks (e.g. Miller, Prendergast & Quirk 1970). Over time, a bar

will rotate about the center of its galaxy, but it will not generally do so at the same rate as the stars in the galaxy, so one cannot associate particular stars with permanent membership of the bar; rather, one should think of the bar as a density wave propagating through the stars of the disk. The absence of a direct link between the rate at which the bar rotates (its “pattern speed”) and the rate at which stars rotate means that the pattern speed cannot be obtained trivially from the streaming motions of the stars. However, Tremaine & Weinberg (1986) showed that these two quantities can be related by invoking the continuity equation (which merely imposes the constraint that stars should not disappear or appear as they orbit around galaxy). They thus showed that

$$\Omega_p \sin i \int_{-\infty}^{\infty} Ix \, dx = \int_{-\infty}^{\infty} I\bar{v}_{\text{los}} \, dx, \quad (1)$$

where Ω_p is the pattern speed of the bar (in radians per year, or, more commonly, $\text{km s}^{-1} \text{kpc}^{-1}$), i is the inclination of the galaxy, \bar{v}_{los} is the mean streaming velocity of the stars at each point in the disk, I is the surface brightness at each point, and the integrals are carried out along any line parallel to the galaxy’s major axis. Hence, if we denote the intensity-weighted averages of x and \bar{v}_{los} along lines parallel to the major axis as $\langle x \rangle$ and $\langle \bar{v}_{\text{los}} \rangle$ respectively, we find that $\Omega_p \sin i \langle x \rangle = \langle \bar{v}_{\text{los}} \rangle$. If we calculate $\langle x \rangle$ and $\langle \bar{v}_{\text{los}} \rangle$ for a series of lines parallel to the galaxy’s major axis, then a plot of one against the other should yield a straight line of slope $\Omega_p \sin i$. Using the apparent axial ratio of the galaxy disk at large radii (where it is assumed to be intrinsically round), we can estimate i , and hence solve for Ω_p .

Although elegantly simple in principle, the practical implementation of this Tremaine–Weinberg algorithm has proved difficult. For a start, if a galaxy contains significant regions of on-going star formation, then the continuity equation upon which the method relies is not valid, as the quantity of stars (and, more importantly, the amount of light they produce) is not conserved as they travel around the galaxy. Second, the presence of patchy extinction due to dust in the galaxy will alter the amount of light that we receive from a star at different points around its orbit, which also invalidates the use of the continuity equation. Finally, the contributions to the integrals in equation (1) from the range $-\infty < x < 0$ are almost canceled by the contributions from $0 < x < \infty$, so Ω_p is given by the ratio of two integrals that are both close to zero. Thus, any noise in the data will be strongly amplified, resulting in large errors in the derived value of Ω_p . Until recently, it has not been possible to reduce the noise in the value of $\langle \bar{v}_{\text{los}} \rangle$ derived from spectra to a point where a meaningful value for Ω_p could be obtained.

The first successful implementation of the Tremaine–Weinberg method was to observations of the SB0 galaxy NGC 936 (Merrifield & Kuijken 1995). An S0 galaxy is well suited to this analysis, as it contains little obscuring dust and no significant star formation. NGC 936 is also ideally oriented, since having the bar at 45 degrees to the major axis (see Figure 2) maximizes the signal in the integrals in equation (1). Using the Multiple-Mirror Telescope, we obtained five sets of spectra with the spectrograph slit oriented parallel to the major axis, as shown in Figure 2. From these data, we obtained the over-all brightness of the galaxy as a function of position along each slit, $I(x)$, from which $\langle x \rangle$ was calculated. We

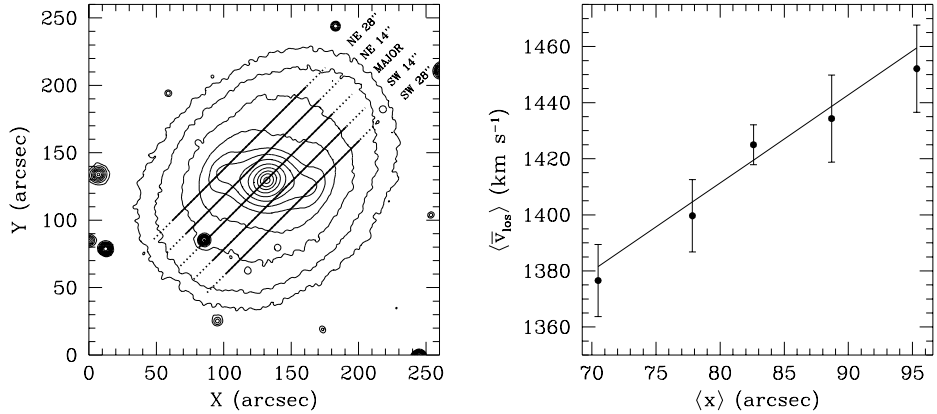


Figure 2. Calculation of the pattern speed of NGC 936. The left panel shows a contour plot of an I-band image of the galaxy overlayed by the positions at which the spectra were obtained. the right panel shows the resulting plot of $\langle \bar{v}_{\text{los}} \rangle$ against $\langle x \rangle$, whose slope is $\Omega_p \sin i$. [Adapted from Merrifield & Kuijken (1995).]

also calculated the line-of-sight velocity distribution of all the stars whose light was admitted by the slit by adding together all the spectra obtained through the slit, and using a deconvolution technique to extract the velocity distribution from the Doppler broadening of the composite spectrum. The quantity $\langle \bar{v}_{\text{los}} \rangle$ is then simply the mean velocity of this integrated distribution. As Figure 2 shows, a plot of $\langle x \rangle$ against $\langle \bar{v}_{\text{los}} \rangle$ for the various slit positions does, indeed, yield a straight line. Combining this slope with the inclination derived from the galaxy's photometry ($i = 41$ deg), we find $\Omega_p = 60 \pm 14 \text{ km s}^{-1} \text{ kpc}^{-1}$.

The success of this calculation confirms the basic picture of a bar as a rotating pattern with a well-defined pattern speed. Indirectly, it also tells us something about the environment in which the bar has formed. In particular, it is instructive to calculate the “co-rotation radius” of the bar, which is the radius at which the stars travel around the galaxy at the same angular speed as the bar pattern. Numerical simulations have shown that when a bar forms, the pattern rotates at such a rate that the co-rotation radius lies just outside the end of the bar. The subsequent evolution of the pattern speed depends on the bar's environment. In isolation, the bar will continue to rotate at this high rate. If, however, the bar is embedded in a massive halo of material, then interactions between the bar and the halo – a form of dynamical friction – will cause the bar to transfer angular momentum to the halo and slow down (Debattista & Sellwood 1998). If one were to calculate the co-rotation radius of such a decelerated bar, one would find that it lay well beyond the end of the bar.

When one combines the derived value of Ω_p with the rate of stellar rotation as a function of radius for NGC 936, one finds that the co-rotation radius lies just beyond the end of the photometric bar. Thus, unless we have caught this bar exceptionally soon after it formed, we can conclude that it cannot be embedded in a dense massive halo.

This conclusion is intriguing because recent cosmological simulations have suggested that if the Universe is dominated by cold dark matter, then the galaxy-scale dark matter halos that condense from this material should have a common centrally-concentrated mass distribution (Navarro, Frenk & White 1997). A disk galaxy forming in such a centrally-concentrated halo would contain a great deal of dark matter at small radii, and so dynamical friction would rapidly decelerate any bar that it might contain. If NGC 936's rapidly-rotating bar turns out to be a common phenomenon, the cosmologists will have to think again.

3. Disk Heating in NGC 488

As a second example of what can be learned about galactic evolution from stellar kinematics, we turn to the phenomenon of disk heating. Although galactic disks are highly-flattened structures, they are not infinitely thin; an edge-on disk galaxy typically has a thickness of some hundreds of parsecs (e.g. van der Kruit & Searle 1981). This thickness implies that the constituent stars must possess random motions perpendicular to the plane of the galaxy, which result in the observed vertical excursions. Spectral observations of face-on galaxies (e.g. van der Kruit & Freeman 1986) confirm the presence of such random motions, as the absorption lines in such spectra are typically Doppler broadened with dispersions of a few tens of kilometers per second. The amplitude of these random motions decreases steadily with radius, reflecting the weakening gravitational pull toward the plane of the galaxy as the density of the disk declines.

Kinematic observations of edge-on galaxies show that there are similar random motions in the radial and tangential directions within disk galaxies. The situation here is a little more complicated, because the mean streaming velocities of the stars dominate the observable kinematics of edge-on galaxies, and these streaming motions have different line-of-sight components at different points on any line through the galaxy, which also contributes to the total broadening of the spectral lines. Further, the radial and tangential random motions contribute varying amounts to the line-of-sight velocity dispersion at different points along the line of sight. However, once these complexities have been accounted for, we arrive at the same basic picture of radial and tangential random motions with dispersions of a few tens of kilometers per second, which decline with distance from the galactic center (Bottema 1993).

Stars are born in gas clouds, which – due to their collisional nature – follow orbits that are close to circular and lie in the plane of the galaxy. Thus, the random motions that we see in the mature stellar population must have been acquired through some subsequent “heating” process. Two main candidates have been advanced for generating the random motions. The first possibility involves heating by giant molecular clouds. As a star orbits around its galaxy, it will occasionally pass sufficiently close to a massive molecular cloud for it to be gravitationally scattered. Since such a scattering will drive the star and cloud toward energy equipartition, the star will on average be accelerated, increasing its random motions with each such encounter. The second candidate for heating also involves gravitational scattering, but in this case the scattering mass is the density enhancement associated with a spiral arm. Each time that an orbiting

star travels through a spiral arm, it will interact with the high density there, and increase the random component of its motion.

How, then, do we distinguish between these two possible candidates for the heating mechanism? A diagnostic was suggested by Jenkins & Binney (1990), who calculated the efficiency with which these mechanisms scatter the stars in different directions. They showed that if heating by molecular clouds were the dominant process, then the amplitudes of the random motions perpendicular to the plane of a galaxy and those in the radial direction should be related, with dispersions in the ratio $\sigma_z/\sigma_R \sim 0.75$. If, on the other hand, density waves provide the dominant scattering mechanism, then $\sigma_z/\sigma_R \sim 0.5$. The basic reason for this difference is that a star has natural frequencies with which it oscillates about its original circular orbit. In the case of radial motions, this natural frequency amounts to ~ 2 oscillations per complete orbit; the oscillation frequency perpendicular to the plane is much higher. A two-armed spiral will give the orbiting star a kick twice per orbit, which is close to its natural radial frequency, so the amplitude of motions in this direction will grow very efficiently. Vertical motions, with their higher natural frequency, do not enjoy this resonant status, so σ_z/σ_R will be relatively low where spiral density waves are responsible for the heating.

Thus, if we can measure the ratio σ_z/σ_R in a galaxy, we can straightforwardly determine which heating mechanism is responsible for the random motions. There is, of course, a catch: σ_z has only been determined for face-on galaxies, while σ_R has only been measured in inclined systems, so it has not been possible to determine this ratio for any single galaxy. The one exception to this problem is the Milky Way, where combining proper motions of nearby stars with their line-of-sight velocities enables all three components of the velocity distribution in the solar neighborhood to be calculated. In this case, we find $\sigma_z/\sigma_R \sim 0.5$, implying that density waves provide the dominant heating mechanism.

With only one datum, it is difficult to draw any general conclusions. Fortunately, there is a way to measure σ_z/σ_R in other galaxies. If, instead of picking an edge-on or a face-on galaxy, one looks at an intermediate-inclination system, then it is possible to determine all three components of the velocity dispersion, $\{\sigma_R, \sigma_\phi, \sigma_z\}$. Specifically, the line-of-sight velocity dispersion along the major axis of a galaxy at an inclination angle i is given by $\sigma_{\text{maj}}^2(R) = \sigma_\phi^2 \sin^2 i + \sigma_z^2 \cos^2 i$, while that along the minor axis is given by $\sigma_{\text{min}}^2(R) = \sigma_R^2 \sin^2 i + \sigma_z^2 \cos^2 i$. We thus have two independent observable constraints on the three unknown components of the velocity dispersion. To close this system of equations, we need to turn to dynamical theory: since the non-circular orbit of an individual star results in both radial and tangential random motions at different points around the orbit, σ_R and σ_ϕ are not independent quantities. In fact, in the epicycle approximation, they are related by the simple formula,

$$\frac{\sigma_\phi^2}{\sigma_R^2} = \frac{1}{2} \left(1 + \frac{\partial \ln v_c}{\partial \ln R} \right), \quad (2)$$

where $v_c(R)$ is the circular rotation speed (Binney & Tremaine 1987). By combining equation (2) with the observed values of $\sigma_{\text{maj}}(R)$ and $\sigma_{\text{min}}(R)$, we can solve for all three components of the galaxy's intrinsic velocity dispersion.

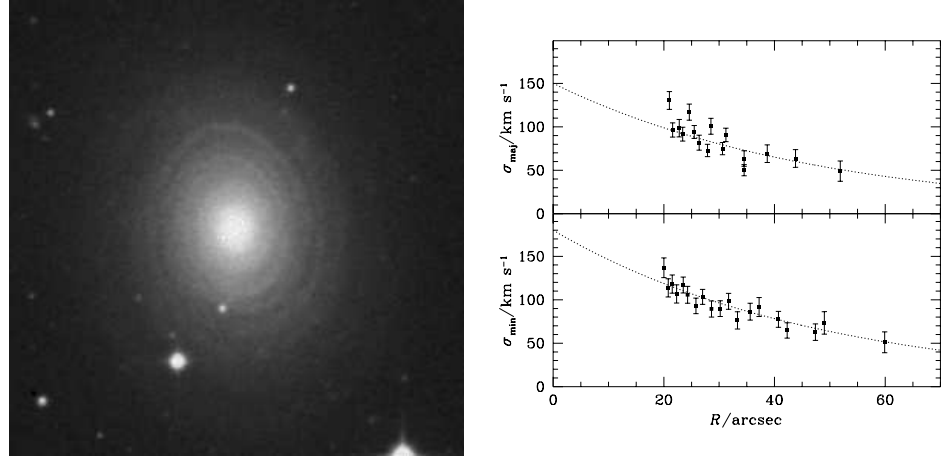


Figure 3. Left panel: image of the moderately-inclined Sa galaxy NGC 488. Right panel: the line-of-sight velocity dispersion measured along its major and minor axes. The dotted line shows the model fit to these dispersion profiles. [Adapted from Gerssen, Kuijken & Merrifield (1997).]

In order to apply this approach, we used the William Herschel Telescope to obtain spectra of the major and minor axes of the moderately-inclined Sa galaxy NGC 488 (Gerssen, Kuijken & Merrifield 1997). Figure 3 shows the line-of-sight velocity dispersions derived from these data. The mean streaming of the stars and emission-line gas provided the values of $v_c(R)$ for equation (2). Combining this equation with the two dispersion profiles, we were able to show that the average velocity dispersions in the three directions lie in the approximate ratio $\sigma_R : \sigma_\phi : \sigma_z \sim 1 : 0.7 : 0.7$.

Unlike the Milky Way, The relatively high value of σ_z/σ_R for NGC 488 seems to favor molecular clouds as the heating mechanism in this galaxy. With hindsight, this difference is not surprising: as befits its early type, NGC 488 does not contain strong spiral structure (see Figure 3), so it is unlikely that heating by spiral density waves will be important in this system. The Milky Way, on the other hand, is a later-type Sbc galaxy (de Vaucouleurs & Pence 1978), where spiral structure will be more significant, explaining the density waves' leading role in heating the stellar population. Thus, we are now in a position to begin to answer the question of what the dominant stellar heating mechanism is in disk galaxies: it appears to vary from system to system.

4. Counter-Rotating Stars in NGC 3593

Having presented one stellar-kinematic project that depended solely on measuring mean streaming motions, and a second that involved measuring the velocity dispersion, we finally turn to a study that requires the analysis of the complete line-of-sight velocity distribution. If one observes the velocity distribution of stars in an edge-on disk galaxy, one would expect to see the signature of rota-

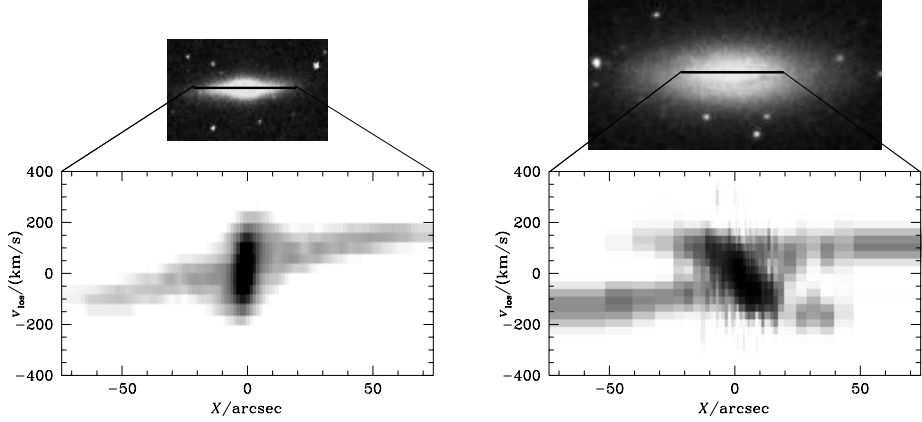


Figure 4. Kinematics along the major axes of edge-on disk galaxies. The axes along which the spectra were obtained are shown in the upper images; the kinematics are shown in the lower plots, with the greyscale showing the projected phase density of stars moving with different line-of-sight velocities at different points along the observed axes. Left Panel: the normal S0 galaxy NGC 7332. Right panel: the kinematically-peculiar Sa galaxy NGC 3593. [Adapted from Binney & Merrifield (1998).]

tion in the data: the stars on one side of the galaxy should be moving towards us (relative to the systemic velocity of the whole galaxy), while those on the other side should be moving away. Close to the center of the galaxy, the light will be dominated by the randomly-orbiting bulge stars, so one would expect to see a larger spread in the velocities in this region, with less sign of rotation. When the line-of-sight velocity distributions of stars are derived from high quality spectra of edge-on galaxies, the vast majority of systems match this description (Kuijken, Fisher & Merrifield 1996) – a typical example is shown in the left panel of Figure 4. There are, however, a few exceptions.

The first kinematically-peculiar stellar disk was discovered by Rubin, Graham & Kenney (1992). They obtained spectra of the apparently-normal edge-on S0 galaxy NGC 4550, and found that at each point away from the center of the galaxy the spectral lines were split into two, one redshifted and one blueshifted relative to the systemic velocity of the galaxy. The interpretation of these data is that NGC 4550 contains two almost identical co-spatial stellar disks that rotate in opposite directions. Since then, a few further examples of this strange phenomenon have been uncovered. Merrifield & Kuijken (1994) found that NGC 7217 contains a retrograde component, but in this case, although the counter-rotating disks are comparable in extent, one contains three times as many stars as the other. Figure 4 shows the further example of NGC 3593, discovered by Bertola et al. (1996), where one of the components is dominant at small radii, but it has a shorter scale-length than the other component, and therefore becomes the fainter at large radii. Although there are now several examples of this phenomenon, it is not common: a systematic survey of 28

S0 galaxies, using spectral data of sufficient quality that even 5% of stars on retrograde orbits would have been detected, failed to find any systems with counter-rotating components (Kuijken, Fisher & Merrifield 1996).

Even though these systems are rare, the existence of a few means that there must be some mechanism by which they are produced. One possibility might be that they form from mergers between disk galaxies that spin in opposite directions. However, simulations show that stellar disks are rather fragile objects, and colliding them invariably destroys the flattened structure, producing an elliptical system (Toomre & Toomre 1972). Disk-like counter-rotating systems must be formed by some more gentle process. One plausible scenario is as follows. A galaxy forms by the conventional mechanism of the gravitational collapse of primordial gas, with a disk forming due to the angular momentum of the infalling material. Over time, the gas disk form stars, creating a conventional galaxy. Primordial gas will continue to rain down on the galaxy, and over time the angular momentum of this infalling material will change. If the angular momentum changes slowly, the orientation of the galaxy will adjust to incorporate the new material. If, however, the angular momentum changes rapidly through close to 180 degrees, the new infalling will collide with any gas left from the initial formation, and the angular momenta of these components will cancel, dumping material toward the center of the galaxy.¹ Once all the first-generation gas has been swept away, subsequent infalling material will be able to create a new gas disk that rotates in the opposite direction to the existing stellar component. Quite a few such disk systems, where the gas and stars orbit in opposite directions, have been documented (Bertola, Buson & Zeilinger 1992). Ultimately, the new gas disk may start to produce stars, resulting in a counter-rotating stellar disk system.

5. Conclusions

Dynamical studies of nearby galaxies have a vital role to play in studying the formation and evolution of these systems. First of all, a galaxy is fundamentally a dynamical entity, so no description of it can be complete without detailed kinematic information. A simulation based on a particular cosmological model may predict the formation of galaxies that look just like those in the real Universe, but if the orbits of the material that makes up these simulated systems do not match those of real galaxies, then the model cannot be correct. Second, once a star is settled on a particular orbit, it is quite hard to shift it elsewhere, so the the dynamical “memories” of these systems can be comparable to the age of the galaxy. Thus, by studying stellar kinematics, one is tapping into the archaeological record of a galaxy’s formation.

The signature of galactic evolution in the stellar kinematics of a galaxy can be quite subtle. Until relatively recently, the quality of data and the sophistication of analysis techniques were not sufficient to unearth these clues. However, as we hope the above examples have illustrated, the quality of kinematic data

¹In this regard, it is interesting that all of the known counter-rotating stellar disks are in early-type galaxies with large bulges – perhaps these bulges owe their stature to the large amount of material dumped on them during the formation process.

now available for stellar disks means that it has become possible to learn a good deal about all aspects of the dynamics of these systems.

We have really only just begun to exploit what is literally a new dimension in the study of galactic structure. In the near future, pilot studies like those described above should lead into large-scale systematic surveys of the stellar-kinematic properties of disk galaxies, providing us with the insights we need to understand the processes by which these systems form and evolve.

Acknowledgments. MRM is currently supported by a PPARC Advanced Fellowship (B/94/AF/1840).

References

- Bertola, F., et al. 1996, *ApJ*, 458, 67
 Bertola, F., Buson, L.M., & Zeilinger, W.W. 1992, *ApJ*, 458, 67
 Binney, J., & Merrifield, M.R. 1998, *Galactic Astronomy*, Princeton: Princeton University Press
 Binney, J., & Tremaine, S. 1987, *Galactic Dynamics*, Princeton: Princeton University Press
 Bottema, R. 1993, *A&A*, 275, 16
 de Vaucouleurs, G., & Pence, W.D. 1978, *AJ*, 83, 1163
 Debattista, V.P., & Sellwood, J.A. 1998, *ApJ*, 493, 5
 Gerhard, O.E. 1993, *MNRAS*, 265, 213
 Gerssen, J., Kuijken, K., & Merrifield, M.R. 1997, *MNRAS*, 288, 618
 Jenkins, A., & Binney, J. 1990, *MNRAS*, 245, 305
 Kent, S.M. 1987, *AJ*, 93, 816
 Kuijken, K., Fisher, D., & Merrifield, M.R. 1996, *MNRAS*, 283, 543
 Kuijken, K., & Merrifield, M.R. 1993, *MNRAS*, 264, 712
 Merrifield, M.R., & Kuijken, K. 1994, *ApJ*, 432, 575
 Merrifield, M.R., & Kuijken, K. 1995, *MNRAS*, 274, 933
 Miller, R.H., Prendergast, K.H., & Quirk, W.J. 1970, *ApJ*, 161, 903
 Navarro, J.F., Frenk, C.S., & White, S.D.M. 1997, *ApJ*, 490, 493
 Rubin, V., Graham, J.A., & Kenney, J.D.P. 1992, *ApJ*, 394, L9
 Sargent, W.L.W., Schechter, P.L., Boksenberg, A., & Shorridge, K. 1977, *ApJ*, 212, 326
 Tonry, J.L., & Davis, M. 1979, *AJ*, 84, 1511
 Toomre, A., & Toomre, J. 1972, *ApJ*, 178, 623
 Tremaine, S., & Weinberg, M.D. 1986, *ApJ*, 282, L5
 van der Kruit, P.C., & Freeman, K.C. 1986, *ApJ*, 303, 556
 van der Kruit, P.C., & Searle, L. 1981, *A&A*, 95, 116
 van der Marel, R.P., & Franx, M. 1993, *ApJ*, 407, 525